

# Moisture increase in response to high-altitude warming evidenced by tree-rings on the southeastern Tibetan Plateau

Jinbao Li<sup>1</sup> · Jiangfeng Shi<sup>2</sup> · David D. Zhang<sup>1</sup> · Bao Yang<sup>3</sup> · Keyan Fang<sup>4</sup> · Pak Hong Yue<sup>1</sup>

Received: 24 December 2015 / Accepted: 23 March 2016 / Published online: 30 March 2016  
© Springer-Verlag Berlin Heidelberg 2016

**Abstract** Rapid warming has been observed in the high-altitude areas around the globe, but the implications on moisture change are not fully understood. Here we use tree-rings to reveal common moisture change on the southeastern Tibetan Plateau (TP) during the past five centuries, and show that regional moisture change in late spring to early summer (April–June) is closely related to large-scale temperature anomaly over the TP, with increased moisture coincident with periods of high temperature. The most recent pluvial during the 1990s–2000s is likely the wettest for the past five centuries, which coincides with the warmest period on the TP during the past millennium. Dynamic analysis reveals that vertical air convection is enhanced in response to anomalous TP surface warming, leading to an increase in lower-tropospheric humidity and effective precipitation over the southeastern TP. The coherent warm-wet relationship identified in both tree-rings and dynamic

analysis implies a generally wetter condition on the southeastern TP under future warming.

**Keywords** Dendrochronology · High-altitude warming · Moisture change · Tibetan Plateau

## 1 Introduction

Marked increase in global temperature has been observed since the early twentieth century (IPCC 2013; Karl et al. 2015). However, this warming is spatially non-uniform, and a large percentage of rapid warming rates are found over the high-altitude regions in addition to the Arctic (Wang et al. 2014a; Pepin et al. 2015). The Tibetan Plateau (TP), for example, experienced a temperature increase of 0.33 °C/decade during 1961–2012, which is roughly 0.13 °C/decade higher than the global average (Yan and Liu 2014). The TP warming rate did not abate during the recent global warming hiatus since 1998 (Yan and Liu 2014; Pepin et al. 2015), suggesting it being a region of robust response to anthropogenic radiative forcing. State-of-the-art climate models projected that rapid temperature increase on the TP will persist throughout the twenty-first century (Rangwala et al. 2013; Su et al. 2013).

The effects of rapid high-altitude warming are dramatic and widespread. On the TP, extensive glacial shrinkage and permafrost degradation have been observed since the beginning of instrumental measurements in the mid-twentieth century, with accelerating rates over recent decades (Kang et al. 2010; Yao et al. 2012; Wu et al. 2013). Meanwhile, earlier thawing and later freezing of soil have occurred, leading to a substantial reduction in the number of frozen days (Li et al. 2012). The length of the growing season has increased at a rate of roughly 3 days per decade during the

**Electronic supplementary material** The online version of this article (doi:10.1007/s00382-016-3101-z) contains supplementary material, which is available to authorized users.

✉ Jinbao Li  
jinbao@hku.hk

- <sup>1</sup> Department of Geography, University of Hong Kong, Pokfulam, Hong Kong
- <sup>2</sup> School of Geographic and Oceanographic Sciences, Institute for Climate and Global Change Research, Nanjing University, Nanjing 210023, China
- <sup>3</sup> Key Laboratory of Desert and Desertification, Cold and Arid Regions Environmental and Engineering Research Institute, Chinese Academy of Sciences, Lanzhou 730000, China
- <sup>4</sup> Key Laboratory of Humid Subtropical Eco-geographical Process (Ministry of Education), College of Geographical Sciences, Fujian Normal University, Fuzhou 350007, China

**Fig. 1** Map of the Tibetan Plateau showing the location of the tree-ring sampling sites (triangle), the Daocheng (DC) and Lijiang (LJ) meteorological station (black circle), and the four scPDSI grid points (open circle) used in this study. The tree-ring sites are as follows: Black triangle denotes the two sites of this study (MX). Blue triangles denote the three moisture-sensitive sites [BM (Fan et al. 2008a), LX (Liu et al. 2012), and LZ (He et al. 2012)]. Red triangles denote the three temperature-sensitive sites [ML (Fan et al. 2008b), BD (Duan and Zhang 2014), and QM (Wang et al. 2014b)]

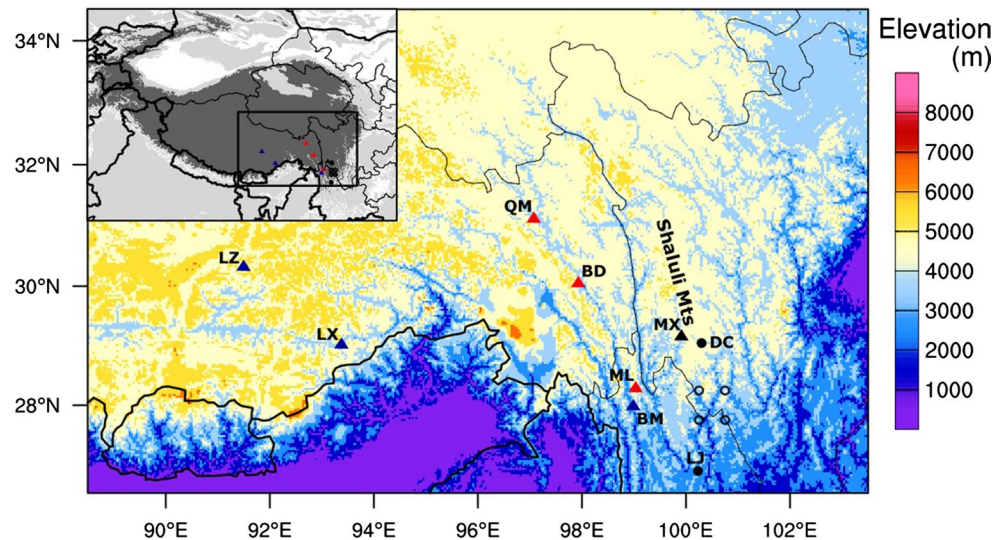


**Table 1** Statistics of the two tree-ring sampling sites, the nearest meteorological station, and the scPDSI grid points developed by van der Schrier et al. (2013)

Data type	Site code	Location (latitude; longitude)	Elevation (m a.s.l.)	Number (core/tree)	Time span (A.D.)
Tree-ring	MAX	29°09'N, 99°56'E	3530	56/28	1509–2006
	MXG	29°09'N, 99°57'E	3600	50/25	1498–2013
Meteorological data	DC	29°03'N, 100°18'E	3728	–	1957–2013
PDSI	–	27°75'–28°25'N, 100°25'–100°75'E	–	–	1944–2012

past half century, largely owing to an earlier start of the growing season (Dong et al. 2012). Interestingly, some plants on the TP delayed the onset of their growth in spring due to rapid winter temperature increase that triggered a later fulfillment of chilling requirements (Yu et al. 2010), although other factors may complicate such an explanation (Chen et al. 2011).

Moisture-related change accompanying rapid warming on the TP is complicated and exhibits considerable spatiotemporal heterogeneity over the past few decades. Seasonally speaking, precipitation has overall increased in winter and spring but decreased slightly in summer and autumn (Li et al. 2010; Chen et al. 2013). Spatially, the annual precipitation has increased in the northeastern and southeastern regions, but decreased in the northwest and the east edge of the TP (Chen et al. 2013; Yang et al. 2014a). Although spatially coherent patterns are found for an increase in evaporation and snow cover and a decrease in surface wind, other factors such as cloud cover, solar radiation and river runoff exhibit large spatiotemporal heterogeneity that complicates moisture change over the TP (Kang et al. 2010; Yang et al. 2014a; Duan and Xiao 2015). As a result, the implications of rapid high-altitude warming on moisture change over the TP are poorly understood, and one critical reason is the lack of extensive, long-term observations (Qiu 2014). Here

we use tree-rings to study common moisture change on the southeastern TP during the past five centuries, and examine whether regional moisture change is related to large-scale TP surface temperature anomaly from a long-term perspective. Tree-rings are employed as a proxy in light of their precise dating, annual resolution, and high sensitivity to climate change in the study area (Fan et al. 2008a; Fang et al. 2010; Liu et al. 2012; Duan and Zhang 2014).

## 2 Data and methods

### 2.1 Tree-ring data

We collected tree-ring samples from two sites in the southern Shaluli Mountains, southeastern TP (Fig. 1). The two sites are close to each other, and both are situated on a steep, leeward slope dominated by subalpine old-growth forests of Forest Fir (*Abies forrestii*). Two increment cores per tree were collected from living trees of *A. forrestii* at breast height (1.3 m above ground). All sampled trees are healthy and relatively isolated, an optimal condition for maximizing climate signals in tree rings. In total 56 cores from 28 trees and 50 cores from 25 trees were retrieved at the site of MAX and MXG, respectively (Table 1).

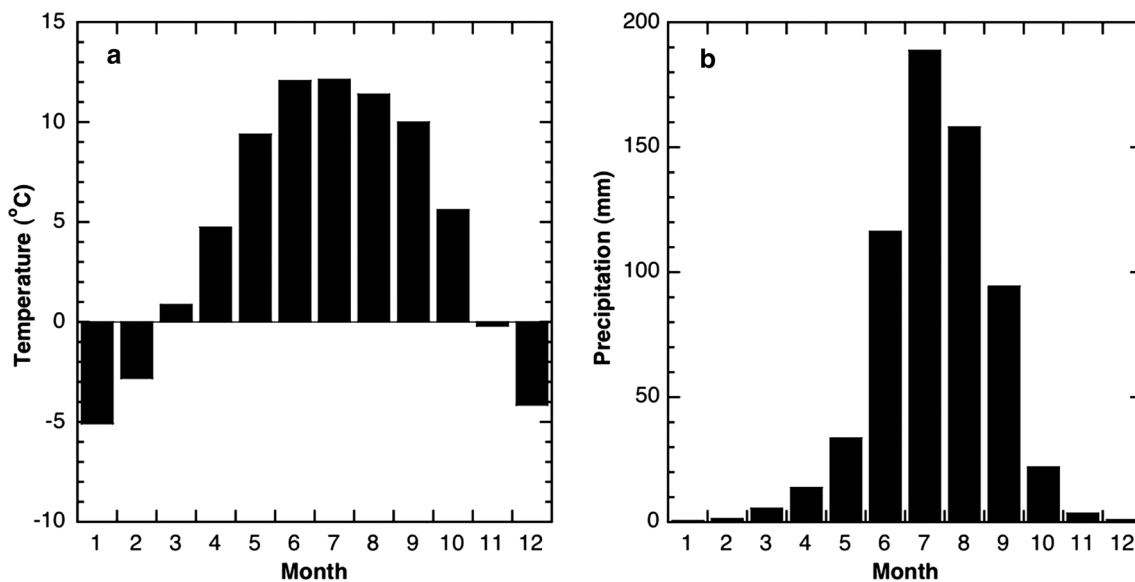


**Fig. 2** **a** Monthly mean temperature and **b** monthly total precipitation records at the Daocheng meteorological station during 1957–2013

After being properly mounted and sanded in the laboratory, all samples were measured using a Velmex ring-width measuring system at 0.001 mm precision. Calendar year was assigned to each growth ring by both visual and the COFECHA program assisted statistical cross-dating methodology (Holmes 1983). Eight (three) cores from the MAX (MXG) site were eliminated during this process due to their irregular growth patterns.

The raw ring-width measurements contain non-climatic growth trends that need to be removed for dendroclimatic study, a procedure termed as “tree-ring standardization” (Fritts 1976). We applied an initial power transformation to reduce the heteroscedastic behavior commonly found in tree-rings (Cook and Peters 1997), and then detrended all series conservatively by fitting negative exponential curves or linear regression curves of any slope. Tree-ring indices were calculated as the residuals between the raw measurements and the fitted curve values, which can effectively avoid potential index value inflation associated with the ratio method (Cook and Peters 1997). The resulting index series were merged to develop a biweight robust mean chronology, with its variance stabilized using the Rbar weighted method (Osborn et al. 1997; Frank et al. 2007). Finally, we applied the “signal-free” approach to mitigate potential trend distortion problem in traditionally detrended chronology (Melvin and Briffa 2008). The resulting “signal-free” chronology was used for further analysis.

## 2.2 Climate data

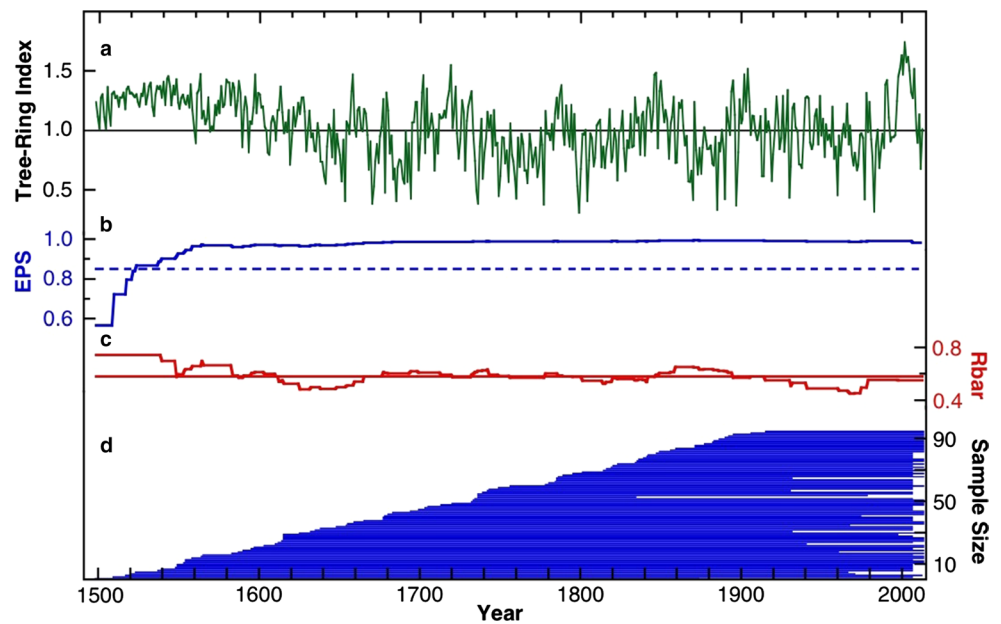
Monthly temperature and precipitation records, spanning 1957–2013, were obtained from Daocheng (DC), the

nearest weather station to our sampling sites (Fig. 2). The half-degree gridded Climatic Research Unit (CRU) TS 3.23 temperature and precipitation datasets (Harris et al. 2014) were used to investigate the spatial relationship of our tree-rings with large-scale climate anomalies. We only used the CRU data starting from 1951, as there were few observations on the TP before the 1950s.

The self-calibrating Palmer Drought Severity Index (scPDSI, van der Schrier et al. 2013) was used as a drought metric. The PDSI is a metric of meteorological drought (Palmer 1965), and has been proven suitable for describing moisture conditions across China (Li et al. 2009a). The scPDSI is a new variant of the PDSI and is more suitable for regions with diverse climatology (van der Schrier et al. 2013). As the nearest Daocheng climate records were not included in the development of the scPDSI dataset, we averaged four half-degree scPDSI grid points relatively close to our sampling sites to represent regional moisture condition (Fig. 1). The four grids were chosen because of their proximity to both our sampling sites and the Lijiang (LJ) weather station, which has the longest observations in the area (i.e., 1944–2012) and was included in the scPDSI calculation.

The European Centre for Medium-Range Weather Forecasts (ECMWF) reanalysis dataset (ERA-Interim, Dee et al. 2011) was used for dynamic analysis. ERA-Interim is a global atmospheric reanalysis product covering the data-rich period from 1979 to the present. ERA-Interim was chosen because of its marked improvements on certain key aspects, such as the representation of the hydrological cycle, the quality of the stratospheric circulation, and the handling of biases and changes in the observing system

**Fig. 3** **a** The composite chronology developed from two sites of *A. forrestii* on the southeastern TP. **b** The running EPS statistics. *Dashed line* denotes the 0.85 cutoff value. **c** The running Rbar statistics. *Horizontal line* denotes the mean value. **d** The corresponding sample size



(Dee et al. 2011). As a result, it performs better than other reanalysis products over the TP (Bao and Zhang 2013).

### 3 Results

A 498- (1509–2006) and 516-year (1498–2013) chronology was developed for the MAX and MXG site, respectively (Table 1). The two chronologies agree very well with each other, with a correlation of 0.67 ( $p < 0.001$ ) and an explained variance of 83.6 % by the first principal component during the common period 1509–2006. Further considering the close location of the two sites and their high environmental homogeneity, we merged all the ring-width index series to develop one composite chronology (hereafter, MX) to represent a regional-scale climate signal. This composite chronology spans from 1498 to 2013, and is composed of 95 cores from 47 trees, with a mean segment length of 291 years (Fig. 3). According to the generally accepted expressed population signal (EPS, Wigley et al. 1984) cut-off value of 0.85, the chronology is considered most reliable during 1523–2013 when sample size exceeds five cores from four trees. The running Rbar ranges from 0.45 around the 1970s to 0.74 around the 1520s with a mean value of 0.58 (Fig. 3). These statistics indicate that the chronology contains fairly strong and stable common signals, and is valid for dendroclimatic studies described below.

As shown in Fig. 4a, statistically significant ( $p < 0.05$ ) positive correlations between tree-rings and precipitation are found in previous August–September and current May–June. Significant positive correlations with temperature are observed from prior October to current April. Negative but non-significant correlations with temperature are found in

current May–June. These results indicate a typical moisture stress on tree growth (Li et al. 2007, 2008; Fan et al. 2009; Fang et al. 2015a). We therefore examined the correlations of tree-rings with the scPDSI during their common period 1944–2012. As shown in Fig. 4b, significant positive correlations with the scPDSI are found in all months investigated, with the highest values in late spring to early summer (April–June). This suggests that the early growing season (EGS) moisture is the most critical factor that limits subalpine tree growth on the southeastern TP.

The above climate–tree growth relationship indicates that our chronology is most suitable for the reconstruction of April–June moisture change in the study area. We used a simple linear regression model to build the reconstruction, and assessed its fidelity by split sample calibration and verification tests (Cook and Kairiukstis 1990). As shown in Table 2, the actual and reconstructed scPDSI correlate at 0.715 during 1944–2012 ( $p < 0.001$ ), which means the reconstruction accounts for 51.2 % ( $R_{\text{adj}}^2 = 50.4$  %) of the actual scPDSI variance during this period. The values of two most rigorous tests of model validation, the reduction of error (RE) and the coefficient of efficiency (CE), are both positive, indicating a good model skill (Cook and Kairiukstis 1990). The results of the sign test, which describes how well the tree-ring estimates track the direction of actual data year to year, exceed the 99 % confidence level. These statistical tests sufficiently validate our regression model. A visual comparison also suggests the reconstruction tracks well the actual scPDSI values at both high- and low-frequency scales, despite that it tends to overestimate the persistence but slightly underestimate the severity of the pluvial condition during the 2000s (Fig. 5). Based on this model we reconstructed April–June moisture

**Fig. 4** Correlations of tree-rings with **a** monthly precipitation (solid bars) and temperature (light bars) records from previous June to current September during 1957–2013, and with **b** monthly scPDSI data during 1944–2012. The dashed lines indicate the corresponding 95 % confidence level

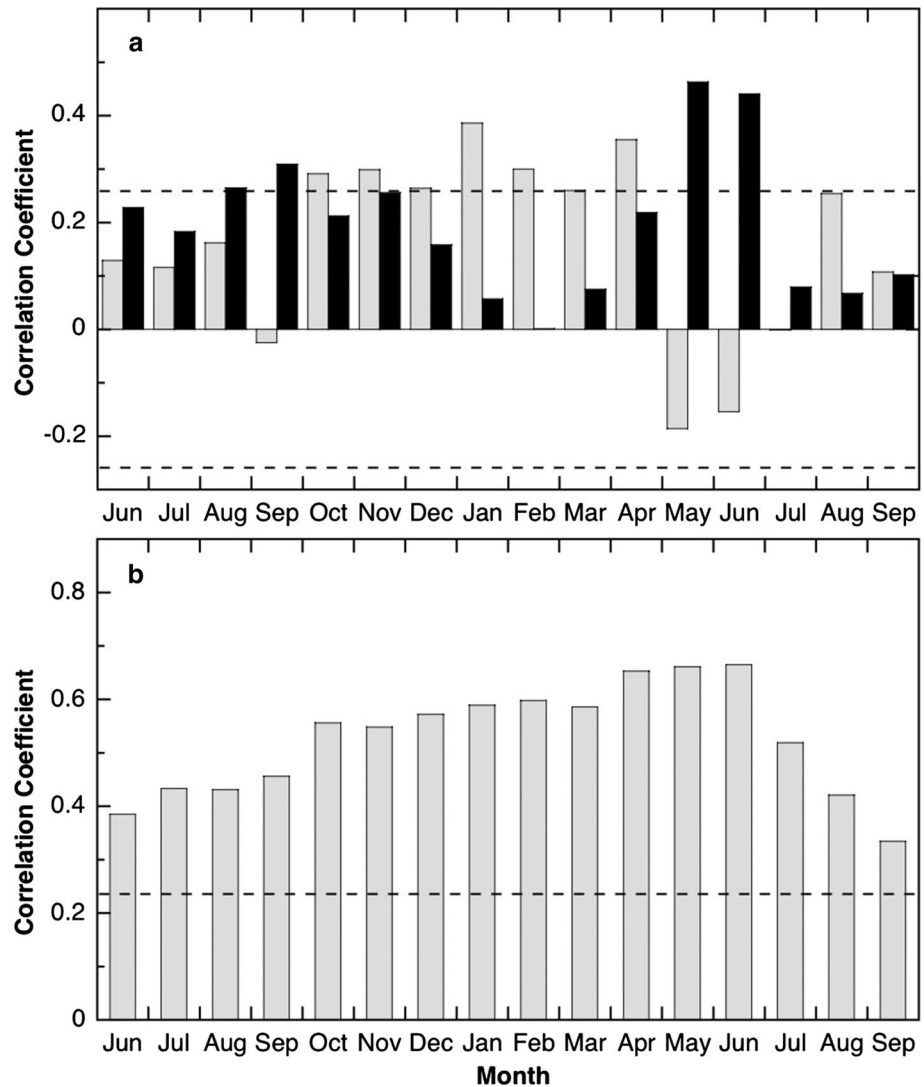


**Table 2** Statistics of calibration and verification test results

	Calibration (1944–1977)	Verification (1978–2012)	Calibration (1978–2012)	Verification (1944–1977)	Full calibration (1944–2012)
r	0.703	0.711	0.711	0.703	0.715
r <sup>2</sup>	0.494	0.506	0.506	0.494	0.512
RE	–	0.461	–	0.561	–
CE	–	0.374	–	0.446	–
Sign test	26/8*	25/10*	27/8*	25/9*	–

\* Significant at  $p < 0.01$

change on the southeastern TP for the past 491 years (Fig. 6a).

#### 4 Discussion

Our results show that subalpine tree growth on the southeastern TP is mainly controlled by the EGS moisture

availability (Fig. 4). This type of climate-tree growth relationship is commonly found over the eastern TP (Li et al. 2008; Fan et al. 2009; Wang et al. 2012; Fang et al. 2015a). Physiological studies revealed that the EGS moisture to a great extent controls the onset of xylogenesis and xylem cell production, and thus largely determines ring formation of subalpine conifers on the eastern TP (Wang et al. 2012; Ren et al. 2015). Significant positive correlations



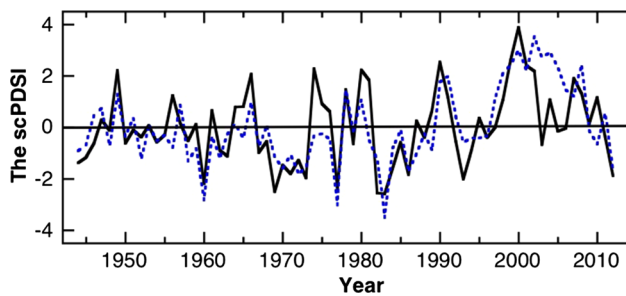


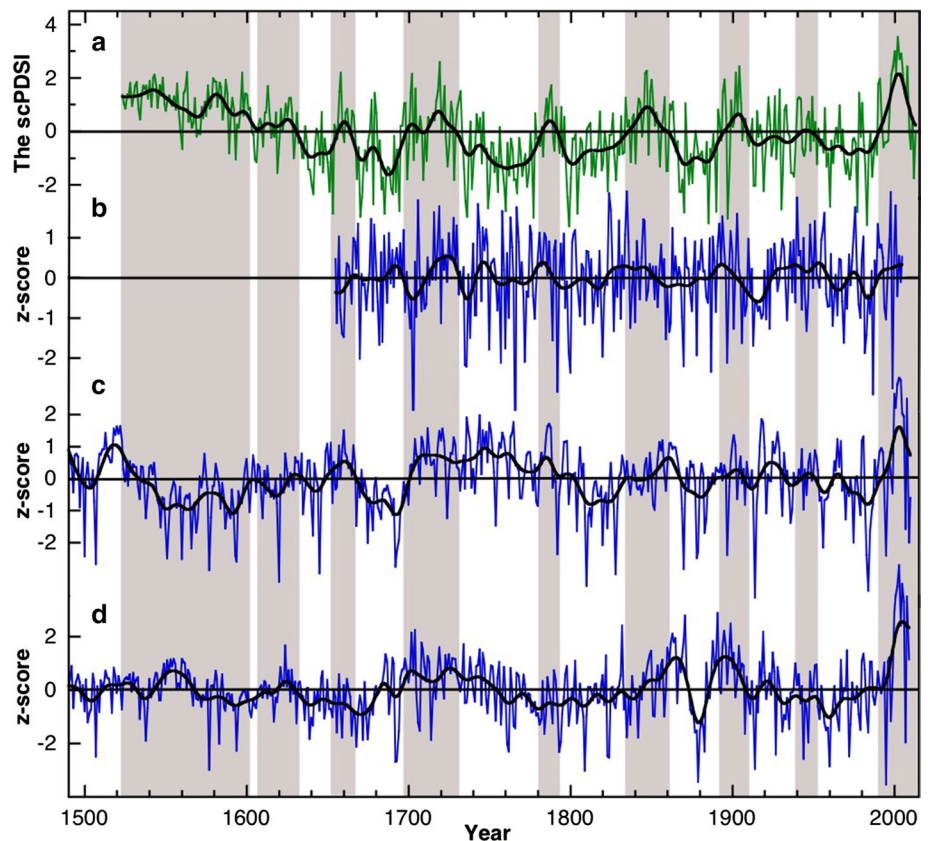
**Fig. 5** Comparison of the actual (*solid line*) and estimated (*dotted line*) April–June scPDSI values during their common period 1944–2012

with precipitation and non-significant negative correlations with temperature in May and June suggest that xylem growth is primarily controlled by precipitation rather than temperature at our sampling sites (Ren et al. 2015). However, at sites where precipitation is more abundant, temperature could be the most critical limiting factor on subalpine tree growth on the southeastern TP (Liang et al. 2010; Yang et al. 2010; Liu et al. 2016). Under that situation, low air and soil temperature may limit tree growth by causing direct leaf and root damage and/or by reducing photosynthetic rate and cambial activity (DeLucia 1986; Gruber et al. 2009; Liang et al. 2009, 2010). Therefore, we caution

that moisture is not necessarily the most critical factor limiting subalpine tree growth across the southeastern TP. Temperature may become most critical when moisture is sufficient for tree growth, and the threshold for such a transition requires future investigation.

Our EGS moisture reconstruction covers the period of 1523–2013 (Fig. 6a). Due to the “segment length curse” (Cook et al. 1995), our reconstruction is capable of resolving interannual to interdecadal moisture variations, but may not be able to represent the centennial-scale variability very well. We therefore focus our discussion on sub-centennial scale moisture variability. As shown in Fig. 6a, our reconstruction reveals marked interdecadal variations in regional EGS moisture over the past five centuries. Severe dry conditions occurred during the 1630s–1640s, 1670s–1690s, 1730s–1770s, 1790s–1820s, 1860s–1880s, 1910s–1930s, and 1950s–1980s, and pronounced wet conditions were observed during the 1520s–1590s, 1610s–1620s, 1700s–1720s, 1830s–1850s, 1890s–1900s, and 1990s–2000s. The most severe and prolonged drought occurred in the 1730s–1770s. The most recent pluvial during the 1990s–2000s was likely the wettest for the past five centuries, although its duration was exceeded by the generally wet conditions during the sixteenth century. It is worth noting that tree-rings overestimated the persistence but slightly underestimated the severity of this pluvial (Fig. 5).

**Fig. 6** Comparison of the EGS scPDSI reconstruction with three tree-ring records that are most sensitive to the EGS moisture condition on the southeastern TP. **a** The April–June scPDSI reconstruction from this study, **b** BM (Fan et al. 2008a), **c** LX (Liu et al. 2012), **d** LZ (He et al. 2012). Data in (b)–(d) have been normalized for direct comparison. *Bold line* in each panel denotes a 21-year low-pass filter. *Vertical shading* denotes wet periods in our reconstruction



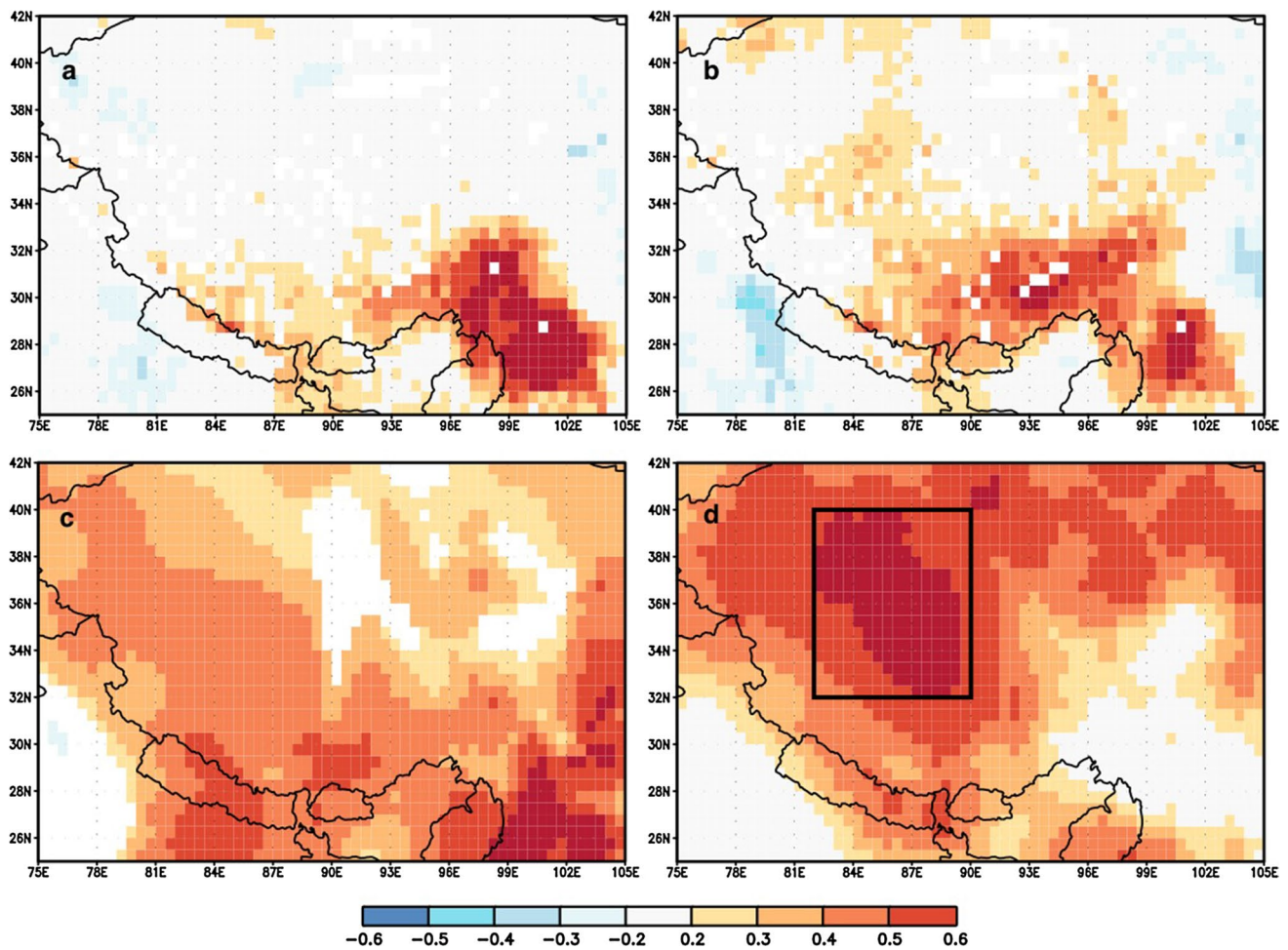


**Fig. 7** Spatial correlation patterns for the period of 1951–2012. **a** Actual and **b** reconstructed April–June scPDSI correlated with regional gridded scPDSI. Reconstructed April–June scPDSI correlated with the CRU minimum temperature in **c** prior winter (October–

February) and **d** current EGS (April–June). The correlation coefficient at the 0.05 significance level is about 0.25, based on a two-tailed Student's *t* test. The *box* in (**d**) denotes the region over which the temperature is averaged

Nonetheless, the 1990s–2000s pluvial is probably unprecedented at least for the past five centuries, as revealed by this and other moisture sensitive tree-rings on the southeastern TP (Fig. 6).

Spatial correlation analysis with instrumental scPDSI during 1951–2012 indicates that our reconstruction is representative of large-scale EGS moisture change on the southeastern TP (Fig. 7a, b). To examine whether it represents large-scale moisture change back in time, we compared our reconstruction with three tree-ring records (BM, LX, and LZ, Fig. 1) that are also most sensitive to the EGS moisture condition on the southeastern TP (Fan et al. 2008a; He et al. 2012; Liu et al. 2012). As shown in Fig. 6, our record agrees well with the other three over most of the past five centuries, with a significant correlation value ( $p < 0.001$ ) of 0.30 with the BM for 1655–2005 (351 years), 0.25 with the LX for 1523–2010 (488 years), and 0.27 with the LZ record for 1523–2009 (487 years).

However, one discrepancy is observed during the sixteenth century when our record indicates a generally wet while the LX record shows a dry condition. We found that our record also shows generally low values if without the “signal-free” adjustment, suggesting that the generally dry condition with the LX record is likely due to the trend distortion introduced by the traditional detrending method (Melvin and Briffa 2008). At any rate, these records exhibit a high degree of coherency with regard to interdecadal variations, indicating common EGS moisture change on the southeastern TP over the past five centuries.

An ensuing question is what caused the coherent EGS moisture change on the southeastern TP. One possibility is the Asian monsoon. However, the EGS is largely ahead of monsoon season (Fig. 2), thus the Asian summer monsoon is unlikely to play a key role. This is corroborated by the non-significant correlations of the actual April–June scPDSI with the East Asian (Li and Zeng 2002) and South Asian

(Wang et al. 2001) summer monsoon indices (Fig. S1). Moreover, both monsoon systems have weakened during recent decades (Yu et al. 2004; Li et al. 2009b; Turner and Annamalai 2012), which is in contrast to the EGS moisture increase on the southeastern TP. Another possibility is the large-scale ocean-atmospheric circulations. However, as shown in Fig. S2, the EGS moisture change on the southeastern TP shows no significant correlation pattern with the precedent or concurrent tropical sea surface temperatures (Rayner et al. 2003), supporting the notion that large-scale ocean-atmospheric circulations do not play a key role on the wetting trend on the TP (Fang et al. 2015b). The third possibility is snow cover on the TP (Estilow et al. 2015). However, the actual April–June scPDSI shows no significant correlation pattern with the precedent winter snow cover on the TP (Fig. S3a). Although it shows significant positive correlations with concurrent snow cover in the study area (Fig. S3b), the covariability more likely suggests a response of snow cover to the EGS moisture availability. The fourth possibility is precipitation on the TP. Similar to snow cover, the actual April–June scPDSI shows no significant correlation pattern with the precedent winter precipitation on the TP (Fig. S3c), suggesting that the latter is not a critical factor that affects the EGS moisture. Instead, it shows significant positive correlations with concurrent precipitation in the study area (Fig. S3d), indicating the EGS moisture is largely determined by precipitation in the same season.

Our moisture reconstruction shows strong and positive correlations with large-scale TP surface temperature anomaly in prior winter (October–February) and current EGS (April–June). The strong and positive correlations with prior winter minimum temperature ( $T_{\min}$ ) are concentrated on the southeastern TP (Fig. 7c), while the correlations with the EGS  $T_{\min}$  are centered over the interior of the TP (Fig. 7d). Similar but weaker correlation patterns are found for the maximum temperature ( $T_{\max}$ ) in both seasons (Fig. S4). The seasonal shift in spatial correlation pattern suggests that temperature of different seasons affects the EGS moisture through different processes. The strong and positive correlations of the EGS moisture with prior winter temperature are found within the study area (Fig. 7c). The atmosphere has a relatively short memory where the climate signals in winter may not be able to exert a time-lagged effect on the warm season moisture, and instead soil moisture is more likely the medium for such a long climate memory (Barnett et al. 1989; Hsu and Liu 2003; Chow et al. 2008). Indeed, we found that the EGS moisture shows persistently high correlations with prior winter scPDSI at our sampling sites (Fig. 4b), consistent with previous studies at other moisture-stressed sites on the southeastern TP (Fan et al. 2008a; Fang et al. 2010; He et al. 2012). These results suggest that prior winter temperature affects the EGS moisture availability by modulating water storage in the soil. In winter, frozen

ground prevents infiltration of snowmelt or rainfall into the soil, leading to higher-than-normal springtime runoff (Niu and Yang 2006). High winter temperature causes thawing of ground and slow melting of snowpack, which result in more infiltration of water into deep soil. Meanwhile, high temperature means more winter precipitation falls as rain instead of snow (Barnett et al. 2005), a change that facilitates winter soil water infiltration. These processes under high winter temperature help retain more water in the local system, which will otherwise be likely lost as surface runoff and river flow during the rapid snow melting in late spring to early summer. The above notion is supported by the observed increase in wintertime low-level clouds at both daytime and nighttime on the TP during recent decades (Duan and Xiao 2015), which is a result of increased surface warming, snowpack melting and evaporation. Overall the increase in wintertime low-level clouds is more pronounced at nighttime than at daytime (Duan and Xiao 2015), supporting our finding that the  $T_{\min}$  is more strongly correlated to the EGS moisture change on the southeastern TP.

The EGS moisture is not strongly related to concurrent  $T_{\min}$  in the study area (Fig. 7d), and its correlation with concurrent  $T_{\max}$  is even negative (Fig. S4b). These results suggest that high EGS temperature leads to regional moisture loss by enhancing evapotranspiration (Fang et al. 2015a; Ren et al. 2015). In contrast, our record shows strong and positive correlations with concurrent surface temperature anomaly over the interior of the TP (Fig. 7d), suggesting that our study area gains moisture when anomalous warming occurs over the interior of the TP. Regression analysis using the ERA-Interim reanalysis data was performed in order to understand the dynamic process. As shown in Fig. 8a, corresponding to positive TP surface temperature anomalies in April–June, positive 200 hPa geopotential anomalies are found over the TP and surroundings, with the center above the interior of the TP with an extension to northwest China. The appearance of strong upper-level anti-cyclone indicates a large-scale upward convection in the region as a response to anomalous surface warming on the TP. The convection leads to an increase in lower tropospheric humidity over the southeastern TP, as represented by positive anomalies of 700 hPa specific humidity (Fig. 8b). In contrast, the convection does not induce more atmospheric humidity over the interior of the TP, largely because the underlying surface is characterized by gobi deserts with limited moisture supply. As a result, strong convection plus increased lower tropospheric humidity lead to an increase in precipitation and effective precipitation [precipitation–evaporation (P–E)] in the southeastern TP, whereas a strong convection plus less lower tropospheric humidity result in a decrease in precipitation and effective precipitation in the interior and western TP (Fig. 8c, d).



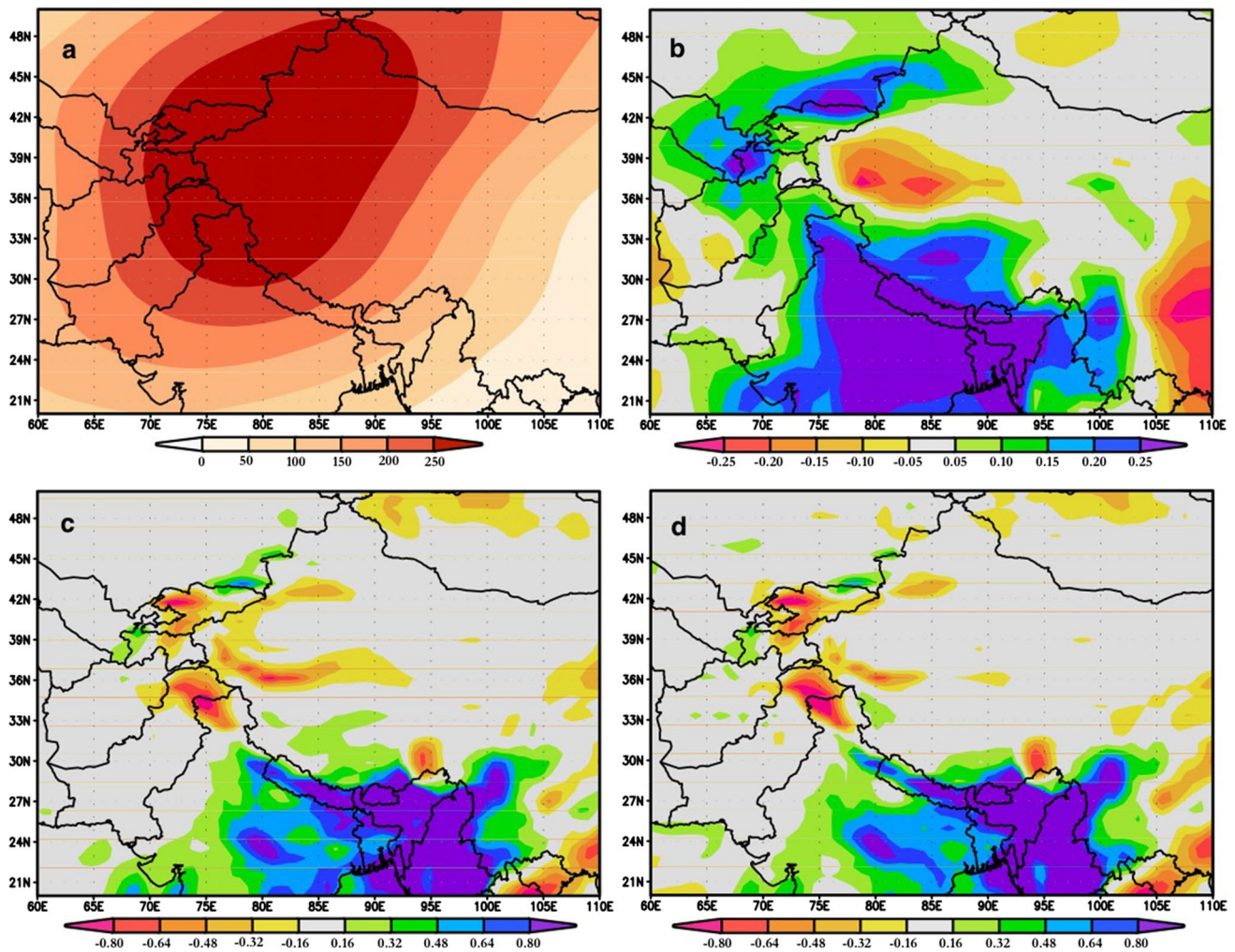


**Fig. 8** Spatial regression patterns for the period of 1979–2014. Regression patterns of **a** 200 hPa geopotential height ( $\text{m}^2/\text{s}^2$ ), **b** 700 hPa specific humidity ( $\text{g}/\text{kg}$ ), **c** precipitation ( $\text{mm}/\text{day}$ ), and **d** effective precipitation ( $P-E$ ,  $\text{mm}/\text{day}$ ) with the interior TP surface

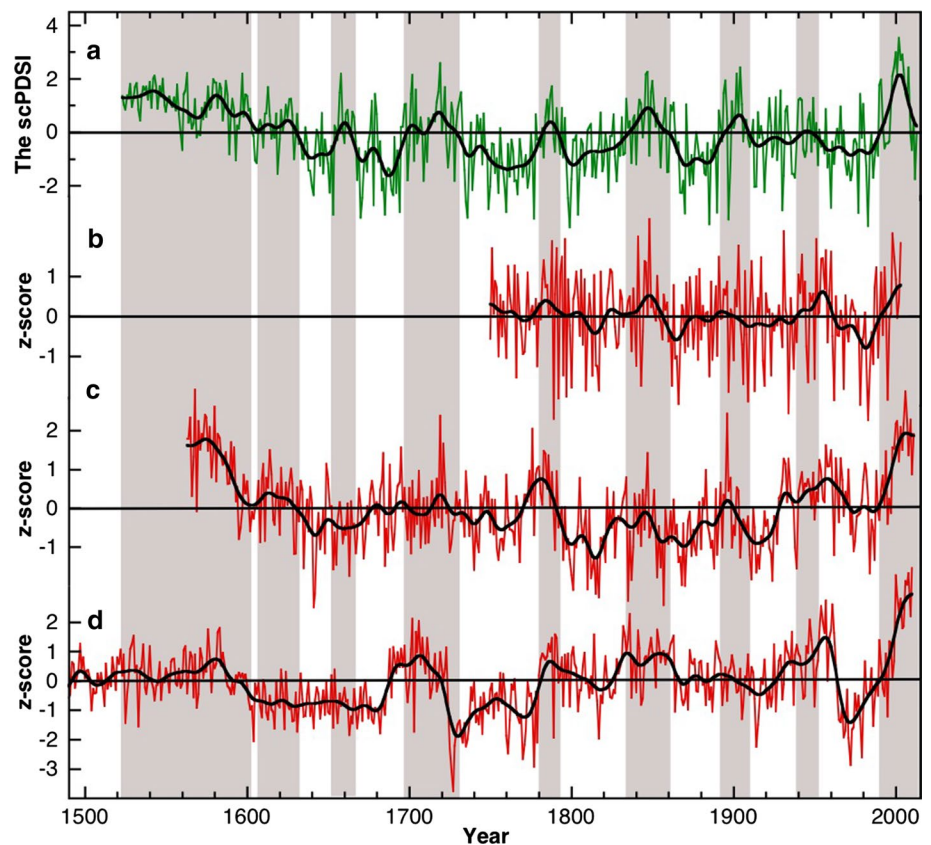
Previous studies found that high temperature leads to strong surface and soil water evaporation that favors the formation of convective precipitation, a crucial process for water supply on the TP before the arrival of monsoon rainfall (Yanai and Li 1994; Lau et al. 2010). This warm-wet relationship has been found in many regions of the TP (Li et al. 2010, 2014; Yang et al. 2014b). Therefore, high EGS surface temperature on the TP benefits moisture supply in its southeastern region through enhancing large-scale evaporation and convective precipitation.

To validate whether the warm-wet relationship has persisted at a long-term scale, we compared our EGS moisture reconstruction with three tree-ring records (ML, BD, and QM, Fig. 1) that represent large-scale temperature change on the TP (Fan et al. 2008b; Duan and Zhang 2014; Wang et al. 2014b). Admittedly only the ML record is from the core area of high correlations shown in Fig. 7c, d. However,

temperature in April–June. The interior TP surface temperature was averaged over a region as denoted in Fig. 7d, using the gridded CRU dataset

it shows very coherent relationship with the other two temperature records (Fig. 9), indicating temperature change is highly uniform on the TP. As shown in Fig. 9, the moisture and temperature reconstructions exhibit a high degree of coherency with regard to their interdecadal variations, with increased moisture coincident with periods of high temperature, and vice versa for the dry and cool periods. In particular, the wettest pluvial of the past five centuries occurred during the 1990s–2000s, which is also the warmest period on the TP during the past millennium (Wang et al. 2014b). The coincidence of the 1990s–2000s warm and pluvial conditions on the southeastern TP may not be enhanced by any persistent trend, as both temperature and moisture records exhibit strong interdecadal variations during the twentieth century (Fig. 9), which is in contrast to the persistent warming and wetting trend on the northeastern TP (Yang et al. 2014b). Therefore, the warm-wet

**Fig. 9** Comparison of the EGS scPDSI reconstruction with three temperature-sensitive tree-ring records on the TP. **a** The April–June scPDSI reconstruction from this study, **b** ML (Fan et al. 2008b), **c** BD (Duan and Zhang, 2014), **d** QM (Wang et al. 2014b). Data in (b)–(d) have been normalized for direct comparison. *Bold line* in each panel denotes a 21-year low-pass filter. *Vertical shading* denotes wet periods in our reconstruction



association on the southeastern TP has persisted at least for the past five centuries.

Our chronology contains prior winter temperature signal (Fig. 4a), which to some extent complicates the interpretation of a warm-wet relationship between the TP surface temperature and the EGS moisture change in its southeastern region. However, two moisture-sensitive chronologies used in the study contain very weak or no prior winter temperature signal (Fan et al. 2008a; Liu et al. 2012) and that exhibit coherent variations with our chronology (Fig. 6), proving that the warm-wet relationship is not due to the inclusion of winter temperature signal in our chronology. At any rate, future sampling of pure moisture-sensitive chronologies on the southeastern TP is needed in order to validate our conclusion. Moreover, the warm-wet relationship breaks down in a few short periods such as the late 1950s to the early 1960s (Fig. 9). Other factors that may affect the EGS moisture change on the southeastern TP await future investigation.

## 5 Conclusions

We developed a 491-year EGS moisture reconstruction with tree-rings, by far the longest for the southeastern TP. Our and other reconstructions together reveal common EGS moisture change on the southeastern TP, and provide

a long-term context for evaluating their relationship with large-scale climate anomaly. Our study indicates a coherent relationship between large-scale TP surface temperature and the EGS moisture change in its southeastern region. High TP surface temperature may affect the EGS moisture supply through the modulation of winter soil water storage and the enhancement of regional EGS evaporation and convective precipitation. State-of-the-art climate models projected that rapid temperature increase on the TP will persist throughout the twenty-first century as a result of continuing anthropogenic greenhouse forcing. The coherent warm-wet association identified in the study implies a generally wetter condition on the southeastern TP under future warming.

**Acknowledgments** This research was funded by the Hui Oi-Chow Trust Fund (No. 201302172004), HKU Seed Funding Program for Basic Research (No. 201309159002), Hong Kong RGC Project (No. 27300514), and the National Science Foundation of China (No. 41271210). Tree-ring data in this study are available on the NOAA paleoclimate database ([www.ncdc.noaa.gov](http://www.ncdc.noaa.gov)).

## References

- Bao X, Zhang F (2013) Evaluation of NCEP–CFSR, NCEP–NCAR, ERA-Interim, and ERA-40 reanalysis datasets against independent sounding observations over the Tibetan Plateau. *J Clim* 26:206–214

- Barnett TP, Dumenil L, Schlese U, Roeckner E, Latif M (1989) The effect of Eurasian snow cover on regional and global climate variations. *J Atmos Sci* 46:661–685
- Barnett TP et al (2005) Potential impacts of a warming climate on water availability in snow-dominated regions. *Nature* 438:303–309
- Chen H, Zhu Q, Wu N, Wang Y, Peng C (2011) Delayed spring phenology on the Tibetan Plateau may also be attributable to other factors than winter and spring warming. *Proc Natl Acad Sci USA* 108:E93
- Chen H et al (2013) The impacts of climate change and human activities on biogeochemical cycles on the Qinghai-Tibetan Plateau. *Glob Change Biol* 19:2940–2955
- Chow KC, Chan JC, Shi X, Liu Y, Ding Y (2008) Time-lagged effects of spring Tibetan Plateau soil moisture on the monsoon over China in early summer. *Int J Climatol* 28:55–67
- Cook ER, Kairiukstis LA (1990) *Methods of Dendrochronology*. Kluwer Academic Press, Dordrecht
- Cook ER, Peters K (1997) Calculating unbiased tree-ring indices for the study of climatic and environmental change. *Holocene* 7:361–370
- Cook ER, Briffa KR, Meko DM, Graybill DA, Funkhouser G (1995) The 'segment length curse' in long tree-ring chronology development for palaeoclimatic studies. *Holocene* 5:229–237
- Dee DP et al (2011) The ERA-Interim reanalysis: configuration and performance of the data assimilation system. *Q J R Meteorol Soc* 137:553–597
- DeLucia EH (1986) Effect of low root temperature on net photosynthesis, stomatal conductance and carbohydrate concentration in Engelmann spruce (*Picea engelmannii* Parry) seedlings. *Tree Physiol* 2:143–154
- Dong M, Jiang Y, Zheng C, Zhang D (2012) Trends in the thermal growing season throughout the Tibetan Plateau during 1960–2009. *Agric For Meteorol* 166:201–206
- Duan A, Xiao Z (2015) Does the climate warming hiatus exist over the Tibetan Plateau? *Sci Rep* 5:13711. doi:10.1038/srep13711
- Duan J, Zhang QB (2014) A 449 year warm season temperature reconstruction in the southeastern Tibetan Plateau and its relation to solar activity. *J Geophys Res* 119:11578–11592
- Estilow TW, Young AH, Robinson DA (2015) A long-term Northern Hemisphere snow cover extent data record for climate studies and monitoring. *Earth Syst Sci Data* 7:137–142
- Fan Z, Bräuning A, Cao K (2008a) Tree ring based drought reconstruction in the central Hengduan Mountains region (China) since A.D. 1655. *Int J Climatol* 28:1879–1887
- Fan Z, Bräuning A, Cao K (2008b) Annual temperature reconstruction in the central Hengduan Mountains, China, as deduced from tree rings. *Dendrochronologia* 26:97–107
- Fan Z, Bräuning A, Cao K, Zhu S (2009) Growth–climate responses of high-elevation conifers in the central Hengduan Mountains, southwestern China. *For Ecol Manag* 258:306–313
- Fang K, Gou X, Chen F, Li J, D'Arrigo R, Cook ER, Yang T, Davi N (2010) Reconstructed droughts for the southeastern Tibetan Plateau over the past 568 years and its linkages to the Pacific and Atlantic Ocean climate variability. *Clim Dyn* 35:577–585
- Fang K, Frank D, Zhao Y, Zhou F, Seppä H (2015a) Moisture stress of a hydrological year on tree growth in the Tibetan Plateau and surroundings. *Environ Res Lett* 10:034010
- Fang K, Makkonen R, Guo Z, Zhao Y, Seppä H (2015b) An increase in the biogenic aerosol concentration as a contributing factor to the recent wetting trend in Tibetan Plateau. *Sci Rep* 5:14620. doi:10.1038/srep14628
- Frank D, Esper J, Cook ER (2007) Adjustment for proxy number and coherence in a large-scale temperature reconstruction. *Geophys Res Lett* 34:L16709. doi:10.1029/2007GL030571
- Fritts HC (1976) *Tree rings and climate*. Academic Press, London
- Gruber A, Wieser G, Oberhuber W (2009) Intra-annual dynamics of stem CO<sub>2</sub> efflux in relation to cambial activity and xylem development in *Pinus cembra*. *Tree Physiol* 29:641–649
- Harris I, Jones PD, Osborn TJ, Lister DH (2014) Updated high-resolution grids of monthly climatic observations—the CRU TS3.10 Dataset. *Int J Climatol* 34:623–642
- He M, Yang B, Bräuning A, Wang J, Wang Z (2012) Tree-ring-derived millennial precipitation record for the southern Tibetan Plateau and its possible driving mechanism. *Holocene* 23:36–45
- Holmes RL (1983) Computer-assisted quality control in tree-ring dating and measurement. *Tree-Ring Bull* 43:69–95
- Hsu HH, Liu X (2003) Relationship between the Tibetan Plateau heating and east Asian summer monsoon rainfall. *Geophys Res Lett* 30:2066. doi:10.1029/2003GL017909
- Intergovernmental Panel on Climate Change (IPCC) (2013) *Climate change 2013: the physical science basis*. Cambridge University Press, Cambridge
- Kang S, Xu Y, You Q, Flügel WA, Pepin N, Yao T (2010) Review of climate and cryospheric change in the Tibetan Plateau. *Environ Res Lett* 5:015101
- Karl TR et al (2015) Possible artifacts of data biases in the recent global surface warming hiatus. *Science* 348:1469–1472
- Lau WKM, Kim MK, Kim KM, Lee WS (2010) Enhanced surface warming and accelerated snow melt in the Himalayas and Tibetan Plateau induced by absorbing aerosols. *Environ Res Lett* 5:025204
- Li J, Zeng Q (2002) A unified monsoon index. *Geophys Res Lett* 29:1274. doi:10.1029/2001GL013874
- Li J, Chen F, Cook ER, Gou X, Zhang Y (2007) Drought reconstruction for north central China from tree rings: the value of the Palmer drought severity index. *Int J Climatol* 27:903–909
- Li J, Cook ER, D'Arrigo R, Chen F, Gou X, Peng J, Huang J (2008) Common tree growth anomalies over the northeastern Tibetan Plateau during the last six centuries: implications for regional moisture change. *Glob Change Biol* 14:1096–2107
- Li J, Cook ER, D'Arrigo R, Chen F, Gou X (2009a) Moisture variability across China and Mongolia: 1951–2005. *Clim Dyn* 32:1173–1186
- Li J et al (2009b) Summer monsoon moisture variability over China and Mongolia during the past four centuries. *Geophys Res Lett* 36:L22705. doi:10.1029/2009GL041162
- Li L, Yang S, Wang Z, Zhu X, Tang H (2010) Evidence of warming and wetting climate over the Qinghai-Tibet Plateau. *Arct Antarct Alp Res* 42:449–457
- Li X, Jin R, Pan X, Zhang T, Guo J (2012) Changes in the near-surface soil freeze–thaw cycle on the Qinghai-Tibetan Plateau. *Int J Appl Earth Obs Geoinf* 17:33–42
- Li J, Xie SP, Cook ER (2014) El Niño phases embedded in Asian and North American drought reconstructions. *Quat Sci Rev* 85:20–34
- Liang EY, Shao XM, Xu Y (2009) Tree-ring evidence of recent abnormal warming on the southeast Tibetan Plateau. *Theor Appl Climatol* 98:9–18
- Liang E, Wang Y, Xu Y, Liu B, Shao X (2010) Growth variation in *Abies georgei* var. *smithii* along altitudinal gradients in the Sygera Mountains, southeastern Tibetan Plateau. *Trees* 24:363–373
- Liu J, Yang B, Huang K, Sonechkin DM (2012) Annual regional precipitation variations from a 700 year tree-ring record in south Tibet, western China. *Clim Res* 53:25–41
- Liu B, Wang Y, Zhu H, Liang E, Camarero JJ (2016) Topography and age mediate the growth responses of Smith fir to climate warming in the southeastern Tibetan Plateau. *Int J Biometeorol*. doi:10.1007/s00484-016-1148-5
- Melvin TM, Briffa KR (2008) A signal-free approach to dendroclimatic standardization. *Dendrochronologia* 26:71–86



- Niu GY, Yang ZL (2006) Effects of frozen soil on snowmelt runoff and soil water storage at a continental scale. *J Hydrometeorol* 7:937–952
- Osborn TJ, Briffa KR, Jones PD (1997) Adjusting variance for sample-size in tree-ring chronologies and other regional-mean time-series. *Dendrochronologia* 15:89–99
- Palmer WC (1965) Meteorological drought. US Weather Bureau Res Paper 45, 58 pp
- Pepin N et al (2015) Elevation-dependent warming in mountain regions of the world. *Nat Clim Change* 5:424–430
- Qiu J (2014) Tibetan plateau gets wired up for monsoon prediction. *Nature* 514:16–17
- Rangwala I, Sinsky E, Miller JR (2013) Amplified warming projections for high altitude regions of the northern hemisphere mid-latitudes from CMIP5 models. *Environ Res Lett* 8:024040
- Rayner NA, Parker DE, Horton EB, Folland CK, Alexander LV, Rowell DP, Kent EC, Kaplan A (2003) Global analyses of sea surface temperature, sea ice, and night marine air temperature since the late nineteenth century. *J Geophys Res* 108:4407. doi:10.1029/2002JD002670
- Ren P, Rossi S, Gricar J, Liang E, Cufar K (2015) Is precipitation a trigger for the onset of xylogenesis in *Juniperus przewalskii* on the north-eastern Tibetan Plateau? *Ann Bot* 115:629–639
- Su F, Duan X, Chen D, Hao Z, Lan C (2013) Evaluation of the global climate models in the CMIP5 over the Tibetan Plateau. *J Clim* 26:3187–3208
- Turner AG, Annamalai H (2012) Climate change and the South Asian summer monsoon. *Nat Clim Change* 2:587–595
- van der Schrier G, Barichivich J, Briffa KR, Jones PD (2013) A scPDSI-based global data set of dry and wet spells for 1901–2009. *J Geophys Res Atmos* 118:4025–4048
- Wang B, Wu R, Lau KM (2001) Interannual variability of Asian summer monsoon: contrast between the Indian and western North Pacific-East Asian monsoons. *J Clim* 14:4073–4090
- Wang Z, Yang B, Deslauriers A, Qin C, He M, Shi F, Liu J (2012) Two phases of seasonal stem radius variations of *Sabina przewalskii* Kom. in northwestern China inferred from sub-diurnal shrinkage and expansion patterns. *Trees* 26:1747–1757
- Wang J, Yang B, Qin C, Kang S, He M, Wang Z (2014a) Tree-ring inferred annual mean temperature variations on the southeastern Tibetan Plateau during the last millennium and their relationships with the Atlantic multidecadal oscillation. *Clim Dyn* 43:627–640
- Wang Q, Fan X, Wang M (2014b) Recent warming amplification over high elevation regions across the globe. *Clim Dyn* 43:87–101
- Wigley T, Briffa KR, Jones PD (1984) On the average value of correlated time series, with applications in dendroclimatology and hydrometeorology. *J Clim Appl Meteorol* 23:201–213
- Wu T, Zhao L, Li R, Wang Q, Xie C, Pang Q (2013) Recent ground surface warming and its effects on permafrost on the central Qinghai-Tibet Plateau. *Int J Climatol* 33:920–930
- Yan L, Liu X (2014) Has climatic warming over the Tibetan Plateau paused or continued in recent years? *J Earth Ocean Atmos Sci* 1:13–28
- Yanai M, Li C (1994) Mechanism of heating and the boundary layer over the Tibetan Plateau. *Mon Weather Rev* 122:305–323
- Yang B, Kang X, Bräuning A, Liu J, Qin C, Liu J (2010) A 622-year regional temperature history of southeast Tibet derived from tree rings. *Holocene* 20:181–190
- Yang B, Qin C, Wang J, He M, Melvin TM, Osborn TJ, Briffa KR (2014a) A 3,500-year tree-ring record of annual precipitation on the northeastern Tibetan Plateau. *Proc Natl Acad Sci* 111:2903–2908
- Yang K, Wu H, Qin J, Lin C, Tang W, Chen Y (2014b) Recent climate changes over the Tibetan Plateau and their impacts on energy and water cycle: a review. *Glob Planet Change* 112:79–91
- Yao T et al (2012) Different glacier status with atmospheric circulations in Tibetan Plateau and surroundings. *Nat Clim Change* 2:663–667
- Yu R, Wang B, Zhou T (2004) Tropospheric cooling and summer monsoon weakening trend over East Asia. *Geophys Res Lett* 31:L22212. doi:10.1029/2004GL021270
- Yu H, Luedeling E, Xu J (2010) Winter and spring warming result in delayed spring phenology on the Tibetan Plateau. *Proc Natl Acad Sci USA* 107:22151–22156